

Article

Hydrological Modeling with Respect to Impact of Land-Use and Land-Cover Change on the Runoff Dynamics in Godavari River Basin Using the HEC-HMS Model

Sunitha Koneti, Sri Lakshmi Sunkara * and Parth Sarathi Roy 

Centre for Earth Ocean and Atmospheric Sciences, University of Hyderabad, Hyderabad 500046, India; sunitha4242@gmail.com (S.K.); psroy13@gmail.com (P.S.R.)

* Correspondence: srilakshmi.ucess@gmail.com; Tel.: +91-40-2313-2669; Fax: +91-40-2301-0152

Received: 23 March 2018; Accepted: 27 May 2018; Published: 30 May 2018



Abstract: Hydrological modeling and the hydrological response to land-use/land-cover changes induced by human activities have gained enormous research interest over the last few decades. The study presented here analyzes the spatial and qualitative changes in the rainfall–runoff that have resulted from the land-cover changes between 1985–2014 in the Godavari River Basin using the Hydrologic Engineering Centre-Hydrologic Modeling System (HEC-HMS) model and remote sensing—GIS (geographic information system) techniques. The purpose of this paper is to analyze the dynamics of land-use/land-cover (LULC) changes for the years 1985, 1995, 2005, and 2014 for the Godavari Basin. The findings reveal an increase of 0.64% of built-up land, a decrease of 0.92% in shrubland, and an increase of 0.56% in waterbodies between 1985–2014. The LULC change detection results between the years 1985–2014 indicated a drastic change in the cropland, forest, built-up land, and water bodies among all of the other classes. The urbanization and agricultural activities are the major reasons for the increase of cropland, built-up land, and water bodies, at the expense of decreases in shrubland and forest. The study had an overall classification accuracy of 92% and an overall Kappa coefficient of 0.9. The HEC-HMS model is used to simulate the hydrology of the Godavari Basin. The analyses carried out were mainly focussed on the impact of LULC changes on the streamflow pattern. The surface runoff was simulated for the year 2014 to quantify the changes that have taken place due to changes in LULC. The observed and the simulated peak streamflow was found to be the same i.e., 56,780 m³/s on 9 September 2014. In the validation part, the linear regression method was used to correlate the observed and simulated streamflow data at the prominent gauge station of the Badrachalam outlet for the Godavari River Basin and give a correlation coefficient value of 0.83. It was found that the HEC-HMS model is compatible and works better for the rainfall–runoff modeling, as it takes into account the various parameters that are influencing the process. The hydrological modeling that was carried out using the HEC-HMS model has brought out the significant impact of LULCC on rainfall–runoff at the Pranhita sub-basinscale, indicating the model’s ability to successfully accommodate all of the environmental and landscape variables. The study indicates that deforestation at the cost of urbanization and cropland expansions leads to decreases in the overall evapotranspiration (ET) and infiltration, with an increase in runoff. The results of the study show that the integration of remote sensing, GIS, and the hydrological model (HEC-HMS) can solve hydrological problems in a river basin.

Keywords: land use/land cover changes; hydrological modeling; Godavari basin; rainfall–runoff modeling; HEC-HMS model

1. Introduction

Water Resources Management is an important and integrated approach that includes all of the hydrological components and their linkages with one another. It is very important to understand and quantify the hydrological components for the efficient planning and management of the water resources. Human modifications such as land cover change, irrigation, etc., bring extreme changes to the hydrological variations. The water and energy fluxes of the earth system are integrated through the hydrological cycle, and in turn, it affects the fluxes of the system. Hence, the land-use/land-cover (LULC) changes have a great role in influencing the hydrological cycle. Over the past several years, remote sensing data have had an active part in mapping the LULC changes in various parts of India [1–12]. Among them, Pooja et al. [7] have quantified the land use/cover of the Gagas watershed in the Almora district using a survey of India topographic sheet from the year 1965 and LISS III satellite data for the year 2008 over a period of 43 years. Rawat et al. [9,10] carried out a study on the land use/land cover of five major towns of Kumaun Himalaya in Uttarakhand (India), and found that the built-up area has sharply increased due to the construction of new buildings in agricultural and vegetation lands. Amin et al. [8] studied the land-use/land-cover mapping of Srinagar city in Kashmir Valley, and observed that significant changes had taken place in the city between 1990–2007.

The LULC changes in and around the river basins bring drastic changes to the environment, both locally and globally. Studies on the consequences of LULC changes on the hydrological cycles have been carried out by [13–15]. It is very important to assess and understand the hydrological components of a river basin and the impact of LULC for its efficient management of water resources. Hence, mathematical hydrological models—namely the lumped, distributed, and semi-distributed models—play a key role. Among all, the semi-distributed models have their parameters partially varying in space, as the basin is divided into a number of smaller sub-basins. For e.g., the Hydrologic Engineering Centre-Hydrologic Modeling System (HEC-HMS), Soil Water Assessment Tool (SWAT), Hydrologiska Byråns Vattenbalansavdelning model (HBV), etc., hydrological modeling using various hydrological models have been successfully applied for various parts of the river basins in India [16–22]. Dadhwal et al. [16] attempted to model the hydrology of the Mahanadi basin using the VIC hydrological model and assessed the land-cover change impacts on the streamflow at different locations along the river. Pakorn Petchprayoon et al. emphasized the impact of land use/land cover in alleviating the flood problem. Durga Rao et al. [17] studied the hydrological modeling of large river catchments on spatial and non-spatial data. Leong et al. [23] used remote sensing, geographic information system (GIS), and hydrological model for rainfall–runoff modeling. Arash Asadi et al. [18] used HEC-HMS in combination with HEC-GeoHMS for rainfall–runoff modeling of a small sub-basin, Delibajak, and the Kabkian basin by adopting the SCS-CN method. Meenu et al. [19] studied the hydrological impacts of climate change in Tunga-Bhadra river basin of India with HEC-HMS and SDSM. Halwatura et al. [24] worked and found that the HEC-HMS model works good for runoff simulation in a tropical catchment. Roy et al. [20] worked on the calibration and validation of the HEC-HMS model for a river basin in Eastern India, and demonstrated that the use of semi-annual parameters improves the hydrological model. Shinde et al. [22] used the HEC-HMS model to simulate rainfall–runoff modeling for the catchment of Wan reservoir, which is a tributary of Purna River. Nirav Kumar et al. [25] studied the rainfall–runoff modeling for the upstream of Hadaf dam, which is located in the middle Gujarat region, and observed that SCS CN loss model produces slightly better results than the initial and constant loss model. Hence, a proper understanding of the rainfall–runoff relation at different scales for the Godavari river basin is important.

Despite this background, an attempt of hydrological modeling for the Godavari Basin using the HEC-HMS model has not been carried out so far. The present study aims to assess the impact of LULC on the availability of water resources in this region. The main objectives of this study are (i) to assess the past and potential land-cover changes between 1985–2005, and prepare the land-use and land-cover map of the year 2014; (ii) detect the land-use and land-cover changes over the past 30 years; (iii) to assess the water resources in Godavari Basin using the HEC-HMS model and compare the output

obtained by the model with the observed ground data such as discharge at the Badrachalam outlet of the basin for the year 2014; and (iv) to study the impact of the LULC change on the rainfall–runoff in the Pranhita watershed, Godavari River Basin.

2. Study Area: The Godavari River Basin

The Godavari River is the largest of all of the peninsular rivers, with a flow length of 1465 km. It has its origin in Sahyadris near Triambakeswar, at an elevation of 1067m in the Nasik district of Maharashtra, and falls into the Bay of Bengal at Antarvedi, East Godavari. The basin occupies 73°26' E to 83°07' E longitudes and 16°16' N to 23°43' N latitudes in the Deccan plateau, with a catchment area of 3,014,503 km² (Figure 1). The basin covers the states of Maharashtra (48.6%), Telangana (18.8%), Madhya Pradesh (10%), Chhattisgarh (10.9%), Orissa (5.7%), Andhra Pradesh (4.5%), and Karnataka (1.4%). The majority of the basin is covered with agricultural land (59.57%), while 3.6% is covered with water bodies. The Godavari Basin receives almost 84% of the annual rainfall on an average during the southwest monsoon, which sets in mid-June and ends by mid-October. The major problem in the basin is the frequent flooding in its lower reaches, as the area is on the coastal zone, which is cyclone-prone. Badrachalam, Kunavaram, and the deltaic portions of the river are prone to floods frequently. The delta areas face drainage congestion due to flat topography. The other major concern faced by the basin is the frequent drying up of the Godavari River in the drier months. The river water is highly alkaline, as the coal-fired power stations nearby dump their huge reserves of ash into the river.

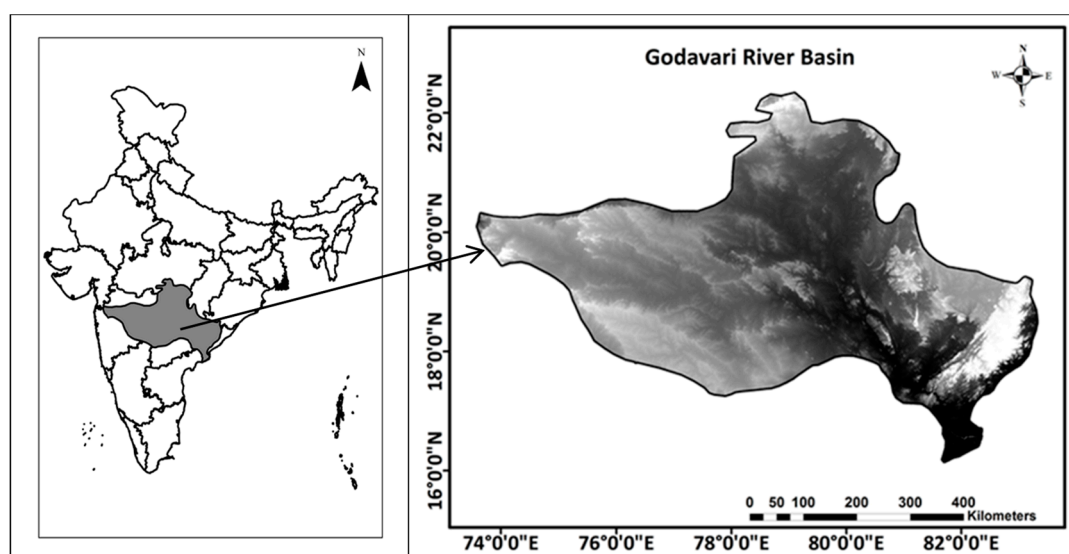


Figure 1. Location map of the study area of the Godavari River basin, covering 73°26' E to 83°07' E longitudes, and 16°16' N to 23°43' N latitudes.

3. Data Used

To find the hydrologic response due to LULC change, the decadal vectorized LULC maps (1985, 1995, and 2005) were obtained from the Indian Space Research Organisation (ISRO) Geosphere Biosphere Programme, soil maps were obtained from NBSS and LUP (Indian National Bureau of Soil Survey and Land Use Planning), and daily rainfall data from the IMD (India Meteorological Department) were used for the study area. The LULC map for the year 2014 that was used in the study was prepared using Landsat 8 Operational Land Imager (OLI) satellite data, which was accessed from Earth Explorer data portal (<https://earthexplorer.usgs.gov/>). For calibration and validation, the daily discharge data was obtained from the Central Water Commission (CWC) for the gauging sites in the basin. ERDAS Imagine and ArcGIS tools were used for preparing the required input data sets in the present study. The soil textural map of the study area at 1:250,000 scales were obtained from

National Bureau of Soil Survey and Land Use Planning, India (NBSS and LUP) in Nagpur. Shuttle Radar Topographic Mission (SRTM) Digital Elevation Model (DEM) data of 30-m resolution was used for extracting the topographic characteristics of the basin. The daily rainfall data was obtained from the Indian Meteorological Department (IMD) for the period of 1985 to 2014 (Figure 2). The basin receives almost 84% of its annual rainfall on average during the southwest monsoon, which sets in mid-June and ends by mid-October. It was found that the rainfall varies temporally and spatially across the basin. The data shows the maximum rainfall (1475 mm during 2013–2014) and minimum (855 mm during 1991–1992) during the last 30 years (1985–2014). HEC-HMS v. 4.2 and HEC-GeoHMS were the tools used for the rainfall–runoff modeling, which were downloaded from the United States Army Corps of Engineers (USACE) website <http://www.hec.usace.army.mil/software/hec-hms>.

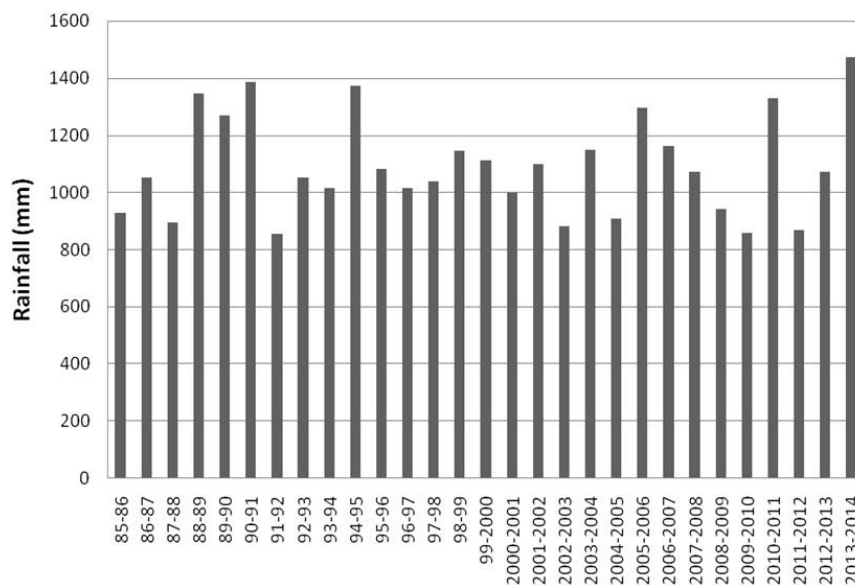


Figure 2. Annual variations in the rainfall of the Godavari Basin.

4. Methodology

4.1. Land-Use and Land-Cover Classification

The satellite remote sensing data, with its repetitive nature, has proved to be quite useful in mapping the LULC patterns and their changes over time. The LULC maps for the Godavari Basin for the years 1985, 1995, and 2005 were obtained from the ISRO Geosphere Biosphere Programme (IGBP) to study the past LULC categories. The LULC classes that were originally present in the 1985, 1995, and 2005 LULC maps were merged, and a new set of LULC classes was created. The new ten (10) LULC classes were: built-up, crop land, forest, plantations, fallow land, shrubland, barren land, water bodies, grassland, and mangroves. The vectorized LULC map for the year 2014 was prepared by means of on-screen visual interpretation and digitization techniques based on interpretation elements at 1:50,000 scale by adopting a standard classification scheme [26] with the help of ERDAS imagine and ArcGIS. The visual interpretation was carried out using on-screen digitization [12]. Finally, the land-cover mapping output was subjected to accuracy assessment.

4.2. Accuracy Assessment

Accuracy assessment is a necessary step to determine and quantify a LULC map. The accuracy assessment was done by comparing the classification product with the reference data, which accurately reflects the true landcover. The accuracy assessment reflects the difference between the classified data and the referenced data. The most common way to represent the classification accuracy of remotely

sensed data is an error matrix [27]. The user and producer accuracy are two widely used measures of accuracy assessment. Producer's accuracy is the percentage of pixels in the reference data for a certain class that are correctly identified by the classifier. User's accuracy is the percentage of pixels classified as a certain class that agree with the reference data. The Kappa coefficient (K) measures the relationship between beyond chance agreement and expected disagreement. The estimate of Kappa is the proportion of agreement after chance agreement is removed from consideration. Kappa statistics/index were computed for a classified map to measure the accuracy of the results. The Kappa coefficient was calculated according to the formula given by [27].

$$\hat{k} = \frac{N \sum_{i=1}^r x_{ii} - \sum_{i=1}^r (x_{i+} \cdot x_{+i})}{N^2 - \sum_{i=1}^r (x_{i+} \cdot x_{+i})}$$

where ' r ' is the number of rows in the matrix, x_{ij} is the number of observations in row i and column j , x_{i+} and x_{+i} are the marginal totals of row i and column i , respectively, and N is the total number of observations [27].

4.3. Land-Use and Land-Cover Change Detection Analysis

Change detection is the process of identifying the differences, if any, in the LULC maps of a river basin. It describes and quantifies the differences between images of the same scene at different times. The important aspect of change detection is to identify and thereby conclude the land-use classes where changes have taken place i.e., a class that has been changed into another class over a period of time. This information is extremely useful for management decisions.

4.4. Hydrological Modeling Using the HEC-HMS Model 4.1

The HEC-HMS model was developed at the Hydrologic Engineering Center (HEC) by the US Army Corps of Engineers. It was designed to simulate the rainfall-runoff processes of dendritic drainage basins. It was also designed to be applicable in a wide range of geographic areas and suitable for simulating daily, monthly, and seasonal streamflow. The HEC-GeoHMS acts as a bridge between the HEC-HMS and ArcGIS (U.S. Army Corps of Engineers 2000, 2001, 2003). The datasets prepared in GeoHMS are directly used in HEC-HMS to simulate the runoff of the basin. HEC-GeoHMS is used to create basin models using a terrain data digital elevation model. By defining a watershed outlet, HEC-GeoHMS automatically delineates the upstream watershed boundary and preliminary sub-basin outlines. GeoHMS creates a basin model that can be imported into HEC-HMS, and also creates a database table of parameters that were estimated from terrain and other supplementary data layers such as soil and land-use databases.

Land use/land cover is a very important parameter in hydrological modeling. The next major component in hydrological model is infiltration. Infiltration depends on soil texture, which in conjunction with the land use provides various basin parameters for the modeling. A soil textural map of the study area at 1:250,000 scale was obtained from National Bureau of Soil Survey and Land Use Planning of India (NBSS and LUP) in Nagpur, and converted into digital format (Figure 3) with the help of ArcGIS; a vector layer of soil map was thus created. The soil textural classes in the present study are clayey, loamy, clay skeletal, loamy skeletal, and outcrops (Figure 3). Among these, the clayey and loamy are the dominating classes that have the properties of low infiltration rate and more runoff. The digital elevation model (DEM) is another main input for the topographic parameter extraction. Shuttle Radar Topographic Mission (SRTM) DEM data of 30-m resolution was used to extract the topographic and hydraulic parameters of the basin. The sub-basins and drainage network are also delineated using the DEM through an automated process. The SRTM-DEM data of 30-m is used for terrain preprocessing, which includes a series of steps starting with filling sinks, flow direction, and flow accumulation, followed by stream definition, stream segmentation, catchment, and drainage

line delineation in HEC-GeoHMS. A new HMS project was created by defining the Badrachalam station as the basin outlet, which includes the delineation of an upstream basin boundary. Keeping the spatial extent of the basin, the computational time, and the desired accuracy, the basin was divided into 145 sub-basins. The basin characteristics such as river length, river slope, and basin slope for each sub-basin were extracted from the DEM.

The soil conservation service curve number (SCS-CN) model was the most widely used in hydrological modeling; it was developed by United States Department of Agriculture (USDA, 1972). In HEC-HMS, for each component of the runoff process, different methods or models are available. Each method has parameters, and the values of these parameters need to be entered as inputs to the model. To compute the losses from the basin, the SCS CN loss method was used, which includes the curve number and percent of imperviousness for each basin. The inputs—the curve number grid and the impervious grid—were prepared using a LULC map, a soil map, and DEM data. The curve number depends upon the hydrological soil group (HSG), land-use type, and AMC-II (antecedent moisture condition). The SCS unit hydrograph transform model is used to compute the direct runoff from excess precipitation. The input parameter for this model is basin lag, which is calculated from the time of concentration for each sub-basin from the excel file generated by the model in the Technical Release 55 (TR55) method. The constant monthly base flow method was used to calculate the base flow, as it represents the amount of ground water that is contributing to the runoff. The base flow for every month has been calculated by means of the straight line method. The Muskingum–Cunge and kinematic wave method were used for routing rivers and channels to the basin outlet, and to estimate the runoff from each sub-basin, the bottom width and side slopes of the reaches are the parameters that are given in the model.

In order to calibrate and validate the model, the model performance is done by (i) visually inspecting and comparing the calculated and observed hydrograph; and (ii) calculating the coefficient of correlation (R^2). For the calibration and validation, the Badrachalam outlet of the Godavari River Basin was taken. By defining the Badrachalam station as the outlet point, the Godavari drainage basin was created, and its topographic characteristics were derived by using SRTM 30-m DEM in HEC-GeoHMS, which is an extension tool bar added to the Arc map. The stream network and sub-basins were delineated; its elevations and channel slopes were derived. The model was run for the year 2014 by using the daily rainfall data, the LULC map, a soil map, and the SRTM 30-m DEM. Runoff was computed for the Godavari River Basin. The result of the modeling process is the computation of stream flow hydrographs at the basin outlet, where the main output from the model is discharge at the outlet of the catchment.

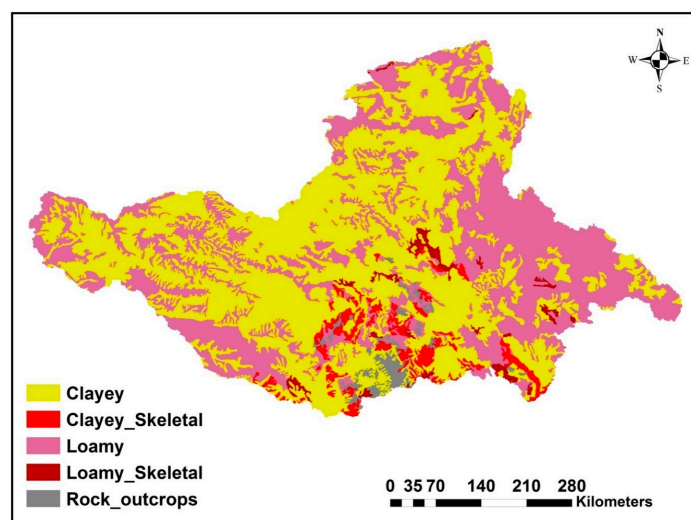


Figure 3. Soil map of the Godavari Basin.

5. Results and Discussion

The hydrological response to human activity-induced land-cover changes in major river basins have gained a lot of attention in the past few years due to their effects on water resources.

5.1. Land-Use and Land-Cover Map of Godavari Basin

A total of 10 classes were mapped in 1985, 1995, 2005, and 2014 for the basin: built-up, cropland, fallowland, plantation, forest, shrubland, grassland, mangrove, barrenland, and waterbodies (Figure 4). The area statistics are presented in the Table 1. The land-use/land-cover maps analyzed from 1985 to 2014 show that the crop land occupies the maximum area—about 58%—in all of the years from 1985 to 2014. The next predominant class found was forest cover, occupying nearly 30% of the basin area. These two land-use classes contribute maximum evapotranspiration to the basin. During 1985–2014 (Figure 4a–d, Table 1), it has been inferred that there was an increase in cropland (from 57.86% in 1985 to 58.33% in 2014), followed by a decrease in forest cover (29.52–29.33%), a decrease in shrubland (5.98–5.06%), an increase in water bodies (3.08–3.24%), an increase in fallow land (2.09–2.15%), an increase in built-up (0.51–1.15%), an increase in plantations (0.50–0.55%), and an increase in grassland (0.02–0.03%). The results indicate that the increase of built-up land and plantation from 1985 to 2014 showed the urbanization and agricultural activities of the people living in this area. The decrease of forest and shrubland was also observed, which might be utilized for agricultural activities. The results revealed that the overall LULC in the basin showed a reverse trend for the forest cover and cropland classes, i.e., decreasing forests and increasing crop land. The expansion of the built up, cropland, and water bodies may be due to the deforestation and loss of shrubland. The area under the mangroves has not undergone any major change, which may be due to the various protection legislations/ordinances formulated by the Government of India. An increase in the fallowland during 1995 was also found, which could be due to adequate rainfall (Figure 2) and the implementation of canal irrigation. The reason of the enhanced agricultural activity could be due to the construction of mini/minor irrigation tanks. Another important increase was found in the built-up land, from 0.51% in 1985 to 1.15% in 2014. A series of changes due to dam and reservoir construction led to deforestation and cropland conversions.

We have evaluated the accuracy of the LULC 2014 map using 825 random points from the total study area, covering 10 random points from all of the classes. We have used the confusion error matrix, which was created with the mapped and ground reference points, to determine the user's accuracy and Cohen's kappa accuracy (Table 2). It has been identified that out of the 825 points, 759 were classified correctly, showing an overall classification accuracy of 92%, and an overall Kappa coefficient of 0.90.

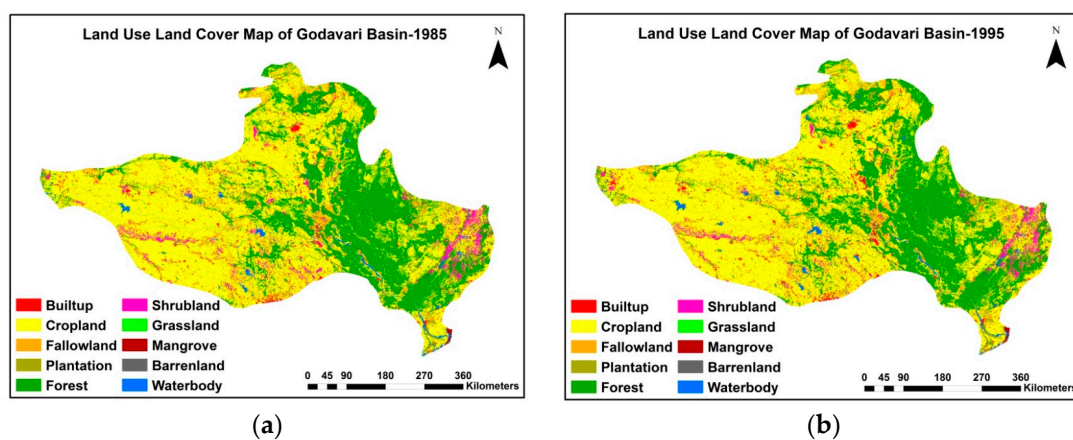


Figure 4. Cont.

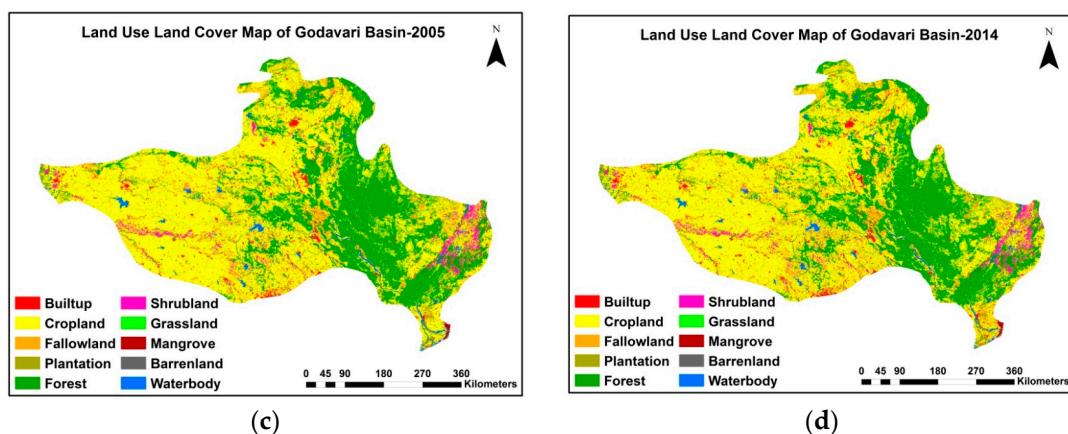


Figure 4. Land use/land cover (LULC) map of the Godavari basin of the years (a) 1985; (b) 1995; (c) 2005 and (d) 2014.

Table 1. Table showing the various land-use/land-cover (LULC) categories of the Godavari River Basin.

LULC Class	1985		1995		2005		2014	
	Area							
	sq-km	%	sq-km	%	sq-km	%	sq-km	%
Builtup	1611	0.51	2253	0.72	2385	0.76	3611	1.15
Cropland	181,962	57.86	182,560	58.05	183,445	58.33	181,337	57.66
Fallowland	6584	2.09	6675	2.12	6860	2.18	6756	2.15
Plantation	1582	0.50	1589	0.51	1590	0.51	1716	0.55
Forest	92,851	29.52	92,361	29.37	92,237	29.33	92,273	29.34
Shrubland	18,808	5.98	17,152	5.45	15,957	5.07	15,907	5.06
Grassland	76	0.02	77	0.02	77	0.02	95	0.03
Mangroves	183	0.06	183	0.06	182	0.06	188	0.06
Barrenland	648	0.21	673	0.21	687	0.22	661	0.21
Waterbodies	10,198	3.24	10,980	3.49	11,083	3.52	11,959	3.80
Total	314,503	100	314,503	100	314,503	100	314,503	100

Table 2. Error matrix or confusion matrix for the accuracy assessment of the LULC map of the Godavari River Basin.

	Reference Data										
	FO	BU	CL	BL	GL	FL	PL	SL	WB	Total	
Classified Data	FO	193	0	2	0	0	0	6	0	0	201
	BU	0	68	2	0	0	2	0	0	0	72
	CL	1	1	137	0	1	0	0	1	8	149
	BL	2	0	6	50	0	0	0	0	1	59
	GL	10	0	4	0	146	0	0	0	0	160
	FL	0	1	0	2	0	25	0	0	0	28
	PL	0	0	1	0	0	5	51	0	0	57
	SL	2	1	4	0	1	0	0	75	0	83
	WB	0	0	1	0	0	0	0	1	14	16
	Total	208	71	157	52	148	32	57	77	23	825

5.2. Change Detection Analysis of the Godavari Basin

The change detection matrices for the change periods of 1985–1995; 1995–2005; and 2005–2014 were calculated, and the results are presented in Tables 3–5, respectively. The land-use/land-cover (LULC) change detection results during 1985 and 2014 also indicated a drastic change in the cropland,

forest, built-up land, and water bodies among all the other classes. The built-up land showed a drastic increase from 1611 to 3611 sq·km. The fallow land and grassland increased from 6584 sq·km to 6756 sq·km and 76 sq·km to 95 sq·km, respectively. The forest area decreased drastically from 92,851 sq·km to 92,273 sq·km. The shrubland area showed a drastic decrease from 18,808 sq·km to 15,907 sq·km. In contrast, the area of water bodies showed an increase from 10,198 sq·km to 11,959 sq·km. The study reveals both negative and positive changes in the land-use/land-cover pattern of Godavari Basin. From the analysis of the rainfall data, it was found that over the last 30 years (1985–1986 to 2013–2014), maximum rainfall (1475 mm during 2013–2014) and minimum (855 mm during 1991–1992) rainfall were recorded, as shown in Figure 2.

Table 3. Change detection matrix of 1985–1995.

		1985									
		BU	CL	FL	PL	FO	SL	GL	MG	BL	WB
1995	BU	1611.30	0.00	0.00	0.00	0.00	0.00	0.00	0.00	0.00	0.01
	CL	325.20	180,662.40	24.46	4.43	9.77	246.01	0.64	0.00	2.45	686.17
	FL	0.01	0.02	6580.79	0.00	0.29	0.14	0.00	0.00	0.00	2.53
	PL	0.00	0.65	0.00	1581.54	0.00	0.00	0.00	0.00	0.00	0.05
	FO	19.38	417.82	4.45	0.17	92,345.13	21.05	0.00	0.00	0.00	42.81
	SL	297.43	1475.48	65.16	2.52	0.00	16,884.76	0.00	0.00	23.45	59.59
	GL	0.00	0.00	0.00	0.00	0.00	0.01	75.95	0.00	0.00	0.00
	MG	0.00	0.00	0.00	0.00	0.00	0.00	0.00	183.12	0.00	0.17
	BL	0.00	0.14	0.00	0.00	0.29	0.08	0.00	0.00	647.54	0.01
	WB	0.00	3.79	0.00	0.13	5.49	0.41	0.00	0.00	0.00	10,188.18

Table 4. Change detection matrix of 1995–2005.

		1995									
		BU	CL	FL	PL	FO	SL	GL	MG	BL	WB
2005	BU	2253.12	0.20	0.00	0.00	0.00	0.00	0.00	0.00	0.00	0.00
	CL	85.98	181,751.03	109.02	1.35	20.22	270.06	0.00	0.15	0.89	321.61
	FL	5.00	60.67	6604.02	0.58	1.51	2.19	0.00	0.90	0.00	0.00
	PL	0.00	3.97	0.00	1578.61	0.59	0.69	0.00	0.13	4.67	0.13
	FO	0.00	153.52	2.62	0.00	92,196.12	0.98	0.00	0.00	0.08	7.64
	SL	31.11	1219.06	135.52	6.33	11.09	15,678.65	0.00	0.00	0.87	69.84
	GL	0.00	0.00	0.00	0.00	0.00	0.00	76.59	0.00	0.00	0.00
	MG	0.02	0.00	1.76	0.01	0.00	0.00	0.00	171.20	0.52	9.62
	BL	0.00	5.30	0.00	0.00	0.00	0.00	0.00	0.00	668.02	0.12
	WB	9.44	251.08	7.33	3.38	7.15	4.93	0.00	9.79	12.05	10,674.38

Table 5. Change detection matrix of 2005–2014.

		2005									
		BU	CL	FL	PL	FO	SL	GL	MG	BL	WB
2014	BU	2383.61	0.00	0.00	0.00	0.00	0.00	0.00	0.00	0.00	1.05
	CL	973.35	180,736.75	76.67	62.30	272.74	58.63	0.26	0.00	21.51	1242.53
	FL	70.01	86.02	6653.40	4.51	0.34	4.66	0.00	0.01	1.83	39.49
	PL	25.01	15.24	0.65	1537.88	4.33	4.21	0.00	0.07	0.00	2.88
	FO	20.94	19.87	5.75	57.82	91,869.15	25.61	22.01	0.00	5.73	209.80
	SL	63.42	30.61	2.46	0.18	17.73	15,761.23	1.40	0.00	15.85	64.61
	GL	0.00	0.91	0.00	0.00	4.08	0.00	71.61	0.00	0.00	0.00
	MG	0.60	0.19	0.52	0.37	0.00	0.00	0.00	173.38	0.00	7.11
	BL	0.64	27.33	0.91	11.09	2.42	23.28	0.00	1.43	603.48	16.53
	WB	73.78	419.87	15.48	42.25	102.00	29.54	0.00	12.78	12.81	10,374.83

The change matrix from 1985 to 2014 shows that mangrove vegetation had a positive change from 1985 to 2014, which may be due to the establishment of the Coringa Wildlife Sanctuary near Kakinada Bay. These positive changes may be due to the active involvement of the government in the

form of protection of natural areas and plantation resorts [28]. These restoration activities are being carried out by MS Swaminathan Research Foundation (MSSRF) jointly with the Andhra Pradesh Forest Department. The increase in water bodies may be due to the construction of dams such as Bhavali, Chanai, Gautami, Kalpathari, Khadakpurna, Lal, Mukane, ShivanTakli, Upper Ghatghar, Upper Manar, and Wakad in Maharashtra; Kosarteda in Chattisgarh; Ragargaon in M.P; Suddavagu in Telangana; etc.

5.3. HEC-HMS Model of the Godavari River Basin

For simulating the runoff of the basin for the year 2014, the LULC map of the year 2014 was reclassified into eight classes: built-up land, cropland, fallow land, plantation, forest, shrubland, barren land, and water bodies. The LULC map for the reclassified classes for the year 2014 was created by ArcGIS (Figure 5).

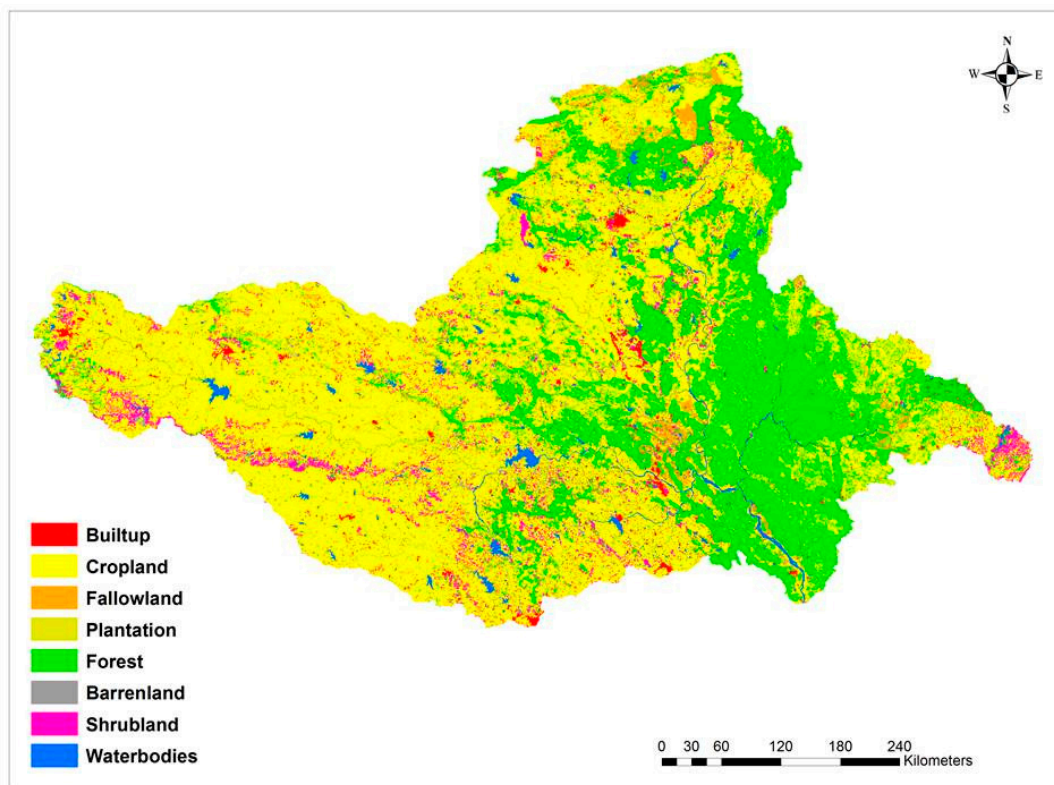


Figure 5. Reclassified land-use/land-cover (LULC) map of the Godavari Basin for the year 2014 showing the various classes of built-up land, cropland, fallow land, plantation, forest, shrubland, barrenland, and waterbodies.

The classified LULC map of the year 2014 (Figure 5) was used for creating the CN grid and an impervious grid. The hydrological soil group is an attribute of the soil mapping unit; each soil mapping unit is assigned a particular hydrological Group: A, B, C, and D. The textural classes were grouped into hydrological soil groups [29]. The study area is covered with groups B, C, and D (Figure 6). Group B soils had a moderately low runoff potential due to moderate filtration rates. Using the hydro DEM (also known as filled DEM), a union of soil and LULC maps, and the CN look-up table, the curve number grid was generated (Figure 7). Curve numbers were assigned by means of the CN look-up table (Table 6) for each land cover mixed with the type of soil [30].

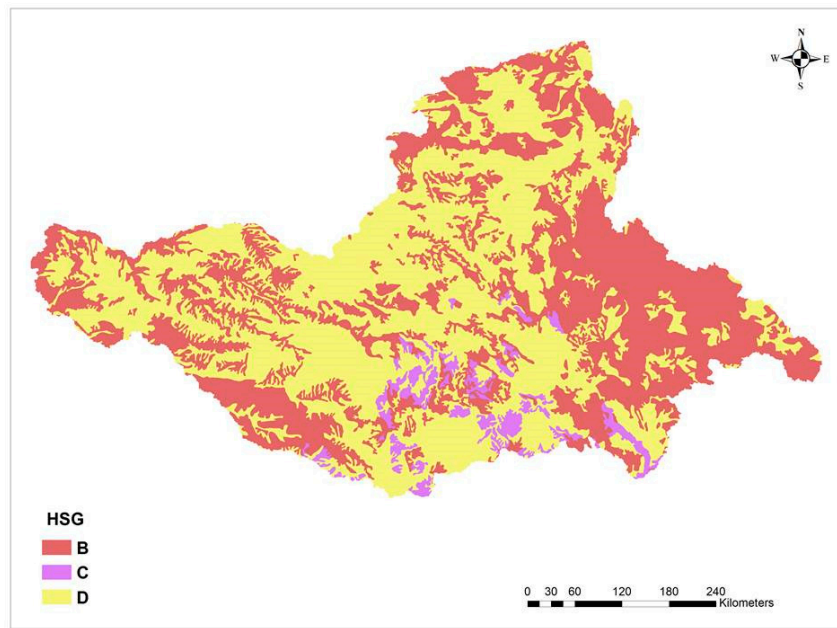


Figure 6. Hydrological soil group map of the study area.

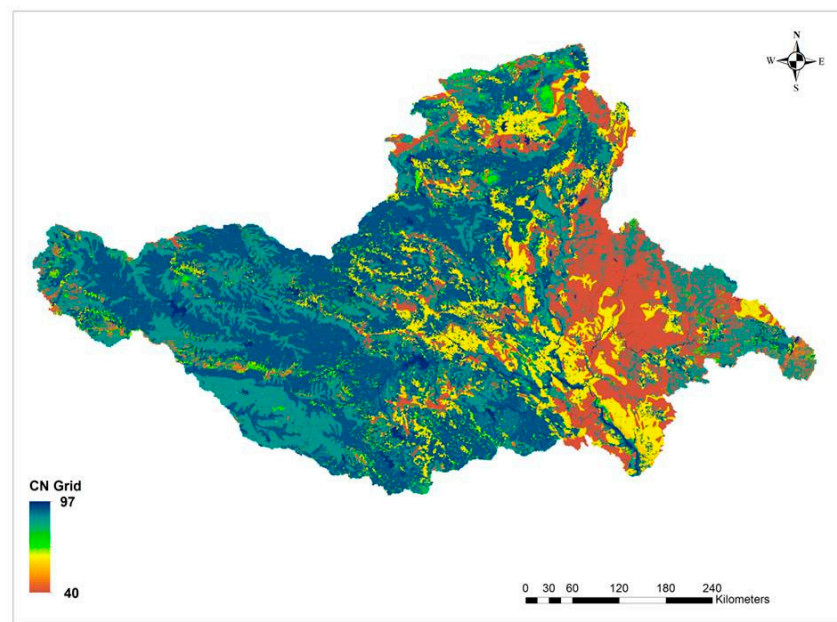


Figure 7. Curve number map of the study area for the year 2014.

Table 6. Curve number look-up table for each land cover type with the type of soil.

LU Value	Description	Soil A	Soil B	Soil C	Soil D
1	Built up	49	69	79	84
2	Cropland	76	86	90	93
3	Fallowland	54	70	80	85
4	Plantation	41	55	69	73
5	Forest	26	40	58	61
6	Shrubland	33	47	64	67
7	Barrenland	71	80	85	88
8	Waterbodies	97	97	97	97

The impervious grid was generated by converting the land-use impervious percent feature to raster [31]. The impervious map was generated, and is shown in Figure 8. These CN values and impervious percent values for each sub-basin were extracted (Table 7). The travel time for each sub-basin was calculated using the TR55 method. The specified hyetograph was considered for the meteorological model, where the daily rainfall data for the year 2014 was given for each sub-basin, and the runoff was simulated at 24 h time interval. The peak discharges were generated for each sub-basin and at the basin outlet. The estimated discharge at the outlet near Bhadrachalam was calibrated against the observed discharge data available from the CWC for the period 2014 (Figure 9). High discharge peaks were observed during the months of July and September. The peak discharge of 56,780 m³/s was simulated for 9 September 2014. The trend of the simulated and observed discharge was verified by the R² value, which was 0.83.

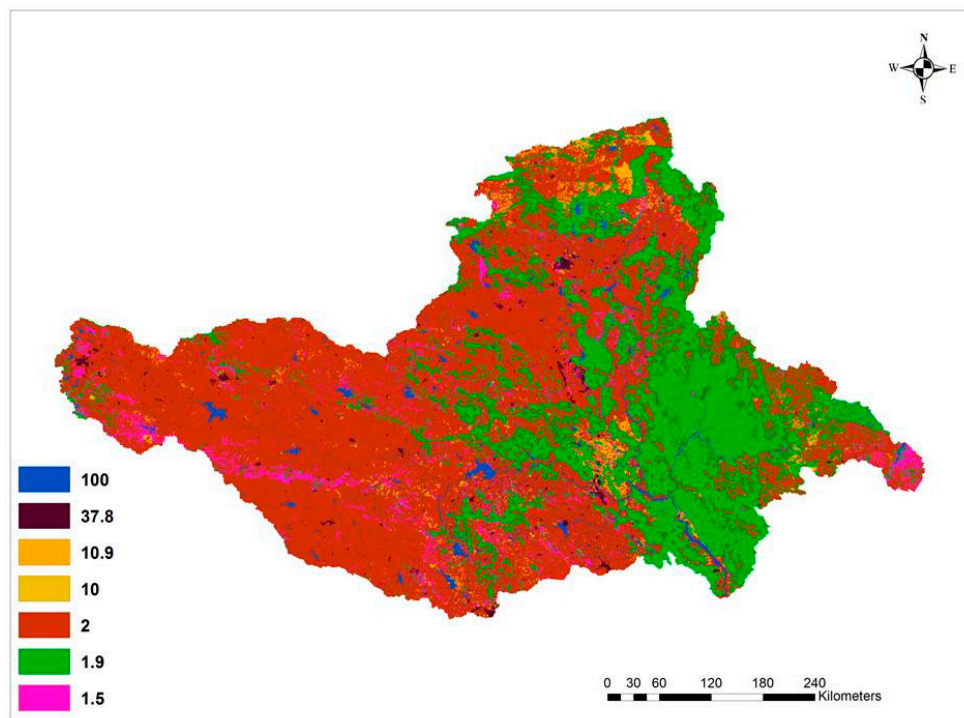


Figure 8. Percent imperviousness map of the study area.

Table 7. The percent imperviousness of the study area for the corresponding land-use classes.

Land Use	% Imperviousness
Builtup	37.8
Cropland	2
Barrenland	10
Forest	1.9
Fallowland	10.9
Plantation	1.9
Shrubland	1.5
Waterbodies	100

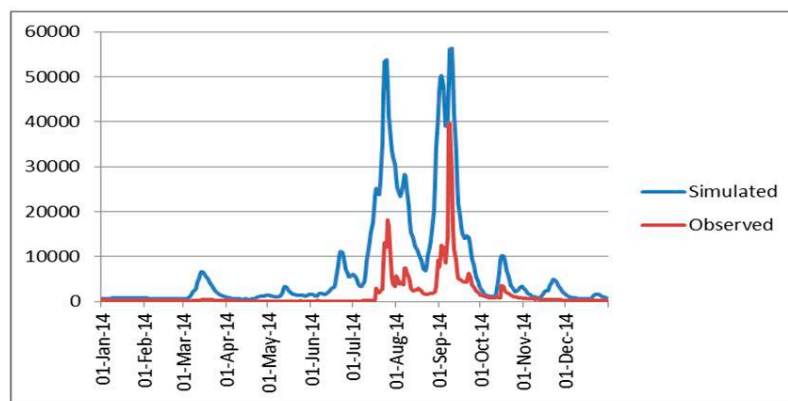


Figure 9. Simulated and observed discharge graph.

5.4. Impact of LULC Change on Runoff

Rainfall is the most important parameter that influences all of the water balance components such as runoff. The total rainfall in the Godavari Basin for the years 1985, 1995, 2005, and 2014 were 928 mm, 1372 mm, 908 mm, and 1474 mm, respectively. The year 1995 had the highest recorded rainfall, and these values are highly correlated with the rainfall. The runoff value depends on the rainfall. The LULC change analysis was carried out for all the watersheds for the years 1985, 1995, 2005, and 2014 and the Pranhita watershed was found to have undergone the major LULC change in terms of decrease in forest cover; decrease in shrubland; increase in built-up land, increase in cropland; increase in fallow land; increase in water bodies; and increase in barren land (Table 8). Hence, we have considered the Pranhita watershed to study the effect of LULC change on the runoff. Simulation for the runoff in the Pranhita watershed was carried out for the years 1985, 1995, 2005, and 2014. Figure 10 shows the distribution of runoff for 1985, 1995, 2005, and 2014 for the Pranhita watershed. The trend of runoff was found to be highly dependable on the amount of rainfall received in the entire basin. The yearly trend of rainfall during 1985 was found to be much less than the other years, and the runoff was also found to follow the same trend (Figures 2 and 10). Similarly, for the year 1995, the runoff was recorded as high, which was mainly due to that year also having the highest rainfall. A decrease in the runoff was observed from 1995 to 2005, which may have been due to the reverse trend in the land-cover conversions and/or human activities. In summary, a decrease in the natural cover of the forest over a period of time caused a significant rise in the surface runoff. The surface runoff increases were due to the decrease in infiltration, and hence groundwater recharge processes. The increase in built-up, which was due to urban expansion and intensive cultivation (increase in cropland), will loosen the soil, leading to soil erosion, as well as a decrease in the surface roughness, and thereby ultimately increase the surface runoff. Urbanization also tend to decrease the infiltration rates, and increase the extent of impervious surfaces, although the area over which such changes have occurred is a small fraction of the total watershed. The HEC-HMS model is particularly suitable for the land-use scenarios and their implications on hydrological processes at regional and global scales over the selected time frames.

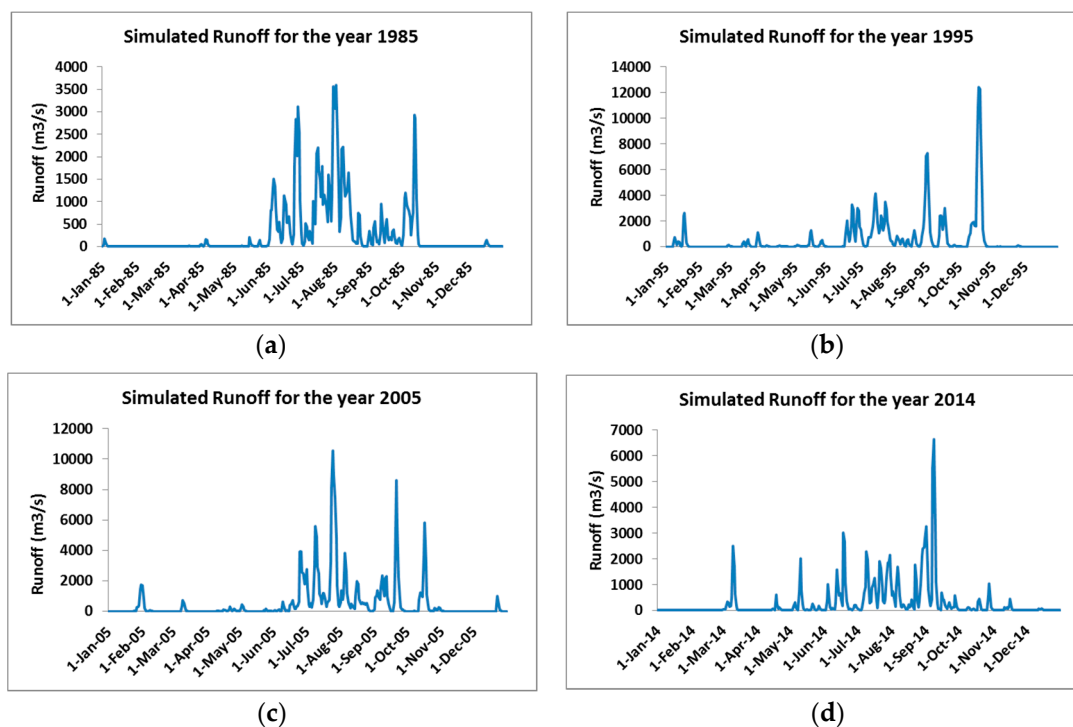


Figure 10. Simulated runoff for the years (a) 1985; (b) 1995; (c) 2005; and (d) 2014 for the Pranhita watershed.

Table 8. Table showing the eight various LULC categories (in sq·km) of the Pranhita sub-basin of the Godavari River Basin.

LULC Class	1985	1995	2005	2014
	Area Sq·Km			
Builtup	128	206	214	323
Cropland	6187	6392	6427	6283
Fallowland	368	367	410	397
Plantation	5	5	5	4
Forest	4451	4307	4306	4298
Shrubland	796	626	554	545
Barrenland	11	11	12	17
Waterbodies	789	821	807	868

6. Conclusions

The study herein is to detect, assess, and predict the trends in the land-use/land-cover changes, and their impact on the surface runoff between 1985 and 2014 in the Godavari Basin. The LULC change detection analysis indicates that the built-up area, fallow land, plantations, grassland, barren land, mangroves, and water bodies of the Godavari Basin have increased, while the area under other categories such as scrub land, crop land, and forest have decreased over the study period from 1985 to 2014 (Figure 4). The study had an overall classification accuracy of 92% and a kappa coefficient of 0.9. The kappa coefficient is rated as substantial, and hence, the classified image was found to be fit for further research.

In addition, an attempt was made to model the hydrology of the Godavari Basin using the HEC-HMS model. The rainfall over the last 30 years in the Godavari Basin had shown drastic changes in the water resources of the Godavari Basin. It was identified that in the smaller regions, the rainfall variability increased. The monsoon rainfall in the Godavari Basin was more variable (17%) than the

all-India monsoon rainfall (11%). The daily rainfall data of the year 2014 were used to simulate the runoff of the basin. The runoff was simulated for 24 h time interval for each year. The peak discharge occurred during July and September. The graph shows that the simulated and observed discharges followed similar trends, with a correlation co-efficient of 0.83. The simulated and observed peak discharges were observed on same date: 9 September 2018.

Although the agreement between the observed and simulated discharges is good, under-estimation and over-estimation are inherent in the simulation. This is because the HEC-HMS model simulates the naturalized flows, and the observed discharge used for validation is based on the human interventions. The model performance showed good agreement at the Bhadrachalam outlet despite the presence of major reservoirs such as Sri Ram Sagar, Indravati, Jayakwadi, and Nizam Sagar, since the calibration was done at this outlet. The model had overestimates ($S > O$) because of the reservoir storage, due to which the observed flows were less than the simulated values. It may be concluded that the agreement between the observed and simulated values largely depends on the land-cover conditions and hydrological components in the basin, as well as their assumptions. The error may be due to the flood plain inundation in the basin.

The hydrological modeling that was carried out in this study using the HEC-HMS model clearly brought out the significant impact of LULC on the hydrological components of runoff on the Pranhita sub-basinscale, indicating the model's ability to successfully accommodate all of the environmental and landscape variables. The overall increase in annual runoff is well corroborated with the overall increase in rainfall from 1985–1995 and 2005–2014, with the conversion of forest to plantation and forest to cropland in the river basins. This study indicates that deforestation at the cost of urbanization and cropland expansions leads to the decrease in the overall ET, with an increase in runoff. This study has provided valuable insights in the perspective of the subsequent changes in hydrological components as a result of LULC for future prediction, which can be useful in developing management policies to conserve the forests in more intelligent and scientific way. Deforestation, cropland expansion, and urbanization are prominent, and will continue in the upcoming decades. This HEC-HMS modeling study can provide insights into future hydrological scenarios, which will offer the planners to take prior actions for sustainable water use.

Author Contributions: P.S.R. has guided and designed the whole research framework. P.S.R. has given the data. S.K. has analyzed the data and carried out the land use land cover analysis and hydrological modeling. S.L.S. has guided, supervised, wrote the paper. S.L.S. and S.K. revised the paper.

Acknowledgments: The authors are grateful for anonymous reviewers for their suggestions in improving the manuscript. We are extremely thankful to Indian Space Research Organization (ISRO) for providing us the LULC data for the periods of 1985, 1995 and 2005 and to carry out this work. We kindly acknowledge USGS for making us available the LANDSAT Data for the year 2014 for carrying out the research work. The authors are thankful to Arpit Chouskey and S.P. Aggarwal, WRD, IIRS, Dehradun, for their support in carrying out the work. The authors are thankful to Sri O. R. K. Reddy, Superintending Engineer, Godavari Circle, Central Water Commission (CWC), Hyderabad, for providing the field data. The authors are grateful to the Head, CEOAS for providing the facilities to carry out this work.

Conflicts of Interest: The authors declare no conflict of interest.

References

1. Gautam, N.C.; Narayanan, L.R.A. Landsat MSS data for land use/land cover inventory and mapping: A case study of Andhra Pradesh. *J. Indian Soc. Remote Sens.* **1983**, *11*, 15–28.
2. Sharma, K.R.; Jain, S.C.; Garg, R.K. Monitoring land use and land cover changes using Landsat imager. *J. Indian Soc. Remote Sens.* **1984**, *12*, 115–121.
3. Brahabhatt, V.S.; Dalwadi, G.B.; Chhabra, S.B.; Ray, S.S.; Dadhwal, V.K. Land use/land cover change mapping in Mahi canal command area, Gujarat using multi-temporal satellite data. *J. Indian Soc. Remote Sens.* **2000**, *28*, 221–232. [[CrossRef](#)]
4. Anil, Z.C.; Katyar, S.K. Impact analysis of open cast coal mines on land use/land cover using remote sensing and GIS technique: A case study. *Int. J. Eng. Sci. Technol.* **2010**, *2*, 7171–7176.

5. Roy, P.S.; Roy, A. Land use and land cover change in India: A remote sensing & GIS perspective. *J. Indian Inst. Sci.* **2010**, *90*, 489–502.
6. Anil, N.C.; Sankar, G.J.; Rao, M.J.; Prasad, I.V.; Sailaja, U. Studies on Land Use/Land Cover and change detection from parts of South West Godavari district, A.P.—Using Remote Sensing and GIS Techniques. *J. Indian Geophys. Union* **2011**, *15*, 187–194.
7. Kamal, P.; Kumar, M.; Rawat, J.S. Application of Remote Sensing and GIS in Land Use and Land Cover Change Detection: A Case study of Gagas Watershed, Kumaun Lesser Himalaya, India. *Quest* **2012**, *6*, 342–345. [[CrossRef](#)]
8. Amin, A.; Fazal, S. Quantification of Land Transformation using Remote sensing and GIS Techniques. *Am. J. Geogr. Inf. Syst.* **2012**, *1*, 17–28. [[CrossRef](#)]
9. Rawat, J.S.; Biswas, V.; Kumar, M. Changes in land use/cover using geospatial techniques: A case study of Ramnagar town area, Nainital district, Uttarakhand, India. *Egypt. J. Remote Sens. Space Sci.* **2013**, *16*, 111–117. [[CrossRef](#)]
10. Rawat, J.S.; Kumar, M. Monitoring land use/cover change using remote sensing and GIS techniques: A case study of Hawalbagh block, district Almora, Uttarakhand, India. *Egypt. J. Remote Sens. Space Sci.* **2015**, *18*, 77–84. [[CrossRef](#)]
11. Sampath Kumar, P.; Mahtab, A.; Roy, A.; Srivastava, V.K.; Roy, P.S.; ISRO, D. Impact of drivers on the Land use/land cover change in Goa, India. In Proceedings of the International Symposium, India Geospatial Forum, Hyderabad, India, 5–7 February 2014.
12. Roy, P.S.; Roy, A.; Joshi, P.K.; Kale, M.P.; Srivastava, V.K.; Srivastava, S.K.; Dwevidi, R.S.; Joshi, C.; Behera, M.D.; Meiyappan, P.; et al. Development of Decadal (1985–1995–2005) Land Use and Land Cover Database for India. *Remote Sens.* **2015**, *7*, 2401–2430. [[CrossRef](#)]
13. Lorup, J.K.; Refsgaard, J.C.; Mazvimavi, D. Assessing the effect of land use change on catchment runoff by combined use of statistical tests and hydrological modelling: Case studies from Zimbabwe. *J. Hydrol.* **1998**, *205*, 147–163. [[CrossRef](#)]
14. Brown, D.G.; Pijanowski, B.C.; Duh, J.D. Modeling the relationships between land use and land cover on private lands in the Upper Midwest, USA. *J. Environ. Manag.* **2000**, *59*, 247–263. [[CrossRef](#)]
15. Seneviratne, S.I.; Corti, T.; Davin, E.L.; Hirschi, M.; Jaeger, E.B.; Lehner, I.; Orlowsky, B.; Teuling, A.J. Investigating soil moisture-climate interactions in a changing climate: A review. *Earth Sci. Rev.* **2010**, *99*, 125–161. [[CrossRef](#)]
16. Dadhwal, V.K.; Aggarwal, S.P.; Mishra, N. Hydrological Simulation of Mahanadi River Basin and Impact of Land Use/Land Cover Change on Surface Runoff Using a Macro Scale Hydrological Model. In Proceedings of the ISPRS TC VII Symposium—100 Years ISPRS, Vienna, Austria, 5–7 July 2010; Volume 38.
17. Rao, K.H.V.D.; Rao, V.V.; Dadhwal, V.K.; Behera, G.; Sharma, J.R. A distributed model for real-time flood forecasting in the Godavari Basin using space inputs. *Int J Disaster Risk Sci.* **2012**, *2*, 31–40. [[CrossRef](#)]
18. Asadi, A.; Sedghi, H.; Porhemat, J.; Babazadeh, H. Calibration, Verification and Sensitivity Analysis of the HEC-HMS Hydrologic Model (Study area: Kabkian Basin and Delibajak Watershed). *Ecol. Environ. Conserv.* **2012**, *18*, 805–812.
19. Meenu, R.; Rehana, S.; Mujumdar, P.P. Assessment of hydrologic impacts of climate change in Tunga-Bhadra river basin, India with HEC-HMS and SDSM. *Hydrol. Process.* **2012**, *27*, 1572–1589. [[CrossRef](#)]
20. Roy, D.; Begum, S.; Ghosh, S.; Jana, S. Calibration and Validation of HEC HMS Model for a River Basin in Eastern India. *ARPN J. Eng. Appl. Sci.* **2013**, *8*, 33–49.
21. Jain, M.; Daman Sharma, S. Hydrological modeling of Vamsadhara River Basin, India using SWAT. In Proceedings of the International Conference on Emerging Trends in Image Processing, Pattaya, Thailand, 15–16 December 2014.
22. Shinde, S.P.; Taley, S.M.; Kale, M.U. Hydrological Modeling with HEC-HMS for Wan Reservoir Catchment. *Int. J. Agric. Sci.* **2016**, *8*, 2263–2266.
23. Leong, T.M.; Ibrahim, A.L.B. *Remote Sensing, Geographic Information System and Hydrological Model for Rainfall—Runoff Modeling*; ResearchGate Publication: Berlin, Germany, 2012.
24. Halwatura, D.; Najim, M.M.M. Application of HEC HMS model for runoff simulation in a tropical catchment. *Environ. Model. Softw.* **2013**, *46*, 155–162. [[CrossRef](#)]
25. Nirav Kumar, K.P.; Mukesh, K.T. Rainfall Runoff Modeling using Remote Sensing, GIS and HEC-HMS model. *J. Water Resour. Pollut. Stud.* **2017**, *2*, 1–8.

26. Anderson, J.R. Land use classification schemes used in selected recent geographic applications of remote sensing. *Photogramm. Eng. Remote Sens.* **1971**, *37*, 379–387.
27. Congalton, R.G.; Green, K. Assessing the accuracy of remote sensed data. *Remote Sen. Environ.* **1999**, *37*, 35–46. [[CrossRef](#)]
28. Reddy, C.S.; Roy, A. Assessment of three decade vegetation dynamics in Mangroves of Godavari delta, India using multi-temporal satellite data and GIS. *Res. J. Environ. Manag.* **2008**, *2*, 108–115.
29. NRCS-USDA. *National Engineering Handbook*; Part 630 Hydrology; Hydrological Soil Groups: Washington, DC, USA, 2009; Chapter 7.
30. Subramanya, K. *Engineering Hydrology*, 4th ed.; McGraw-Hill Education Private Limited: New Delhi, India, 2013.
31. Punng, S. *Estimation of Runoff of an Upper Catchment of an Existing Reservoir by SCS–CN Method Using GIS Software*; IS-030-IA-LSCW: Phnom Penh, Cambodia, 2015; Chapter 3.



© 2018 by the authors. Licensee MDPI, Basel, Switzerland. This article is an open access article distributed under the terms and conditions of the Creative Commons Attribution (CC BY) license (<http://creativecommons.org/licenses/by/4.0/>).